Construction of Membrane Sieves Using Stoichiometric and Stress-Reduced $Si_3N_4/SiO_2/Si_3N_4$ Multilayer Films and Their Applications in Blood Plasma Separation

Dae-Sik Lee, Yo Han Choi, Yong Duk Han, Hyun C. Yoon, Shuichi Shoji, and Mun Youn Jung

The novelty of this study resides in the fabrication of stoichiometric and stress-reduced $Si_3N_4/SiO_2/Si_3N_4$ triple-layer membrane sieves. The membrane sieves were designed to be very flat and thin, mechanically stress-reduced, and stable in their electrical and chemical properties. All insulating materials are deposited stoichiometrically by a low-pressure chemical vapor deposition system. The membranes with a thickness of 0.4 μm have pores with a diameter of about 1 μm. The device is fabricated on a 6" silicon wafer with the semiconductor processes. We utilized the membrane sieves for plasma separations from human whole blood. To enhance the separation ability of blood plasma, an agarose gel matrix was attached to the membrane sieves. We could separate about 1 μL of blood plasma from 5 μL of human whole blood. Our device can be used in the cell-based biosensors or analysis systems in analytical chemistry.

Keywords: Stoichiometric, $Si_3N_4/SiO_2/Si_3N_4$, membrane sieves, plasma separation.

Manuscript received June 29, 2011; revised Oct. 12, 2011; accepted Oct. 27, 2011.

The Si-based devices fabrication was performed at the ETRI CMOS Fab. and MEMS Laboratory. This work was supported by the R&D program of Ministry of Knowledge and Economy (MKE), Rep. of Korea (11ZC1110, Basic Research for the Ubiquitous Lifecare Module Development), and the Priority Research Center Program (2011-0022978) through NRF, Rep. of Korea.

Dae-Sik Lee (phone: +82 42 860 1543, dslee@etri.re.kr), Yo Han Choi (tabby@etri.re.kr), and Mun Youn Jung (myjung@etri.re.kr) are with the IT Convergence Technology Research Laboratory, ETRI, Daejeon, Rep. of Korea.

Yong Duk Han (aj23@ajou.ac.kr) and Hyun C. Yoon (hcyoon@ajou.ac.kr) are with the Department of Molecular Science and Technology, Ajou University, Suwon, Rep. of Korea.

Shuichi Shoji (shojis@waseda.jp) is with the Department of Electronics and Photonic Systems, Waseda University, Tokyo, Japan.

http://dx.doi.org/10.4218/etrij.12.1711.0013

I. Introduction

The passage of individual molecules, cells, or particles through micro/nano-sized pores in membranes is central to many processes in biology [1]-[4]. Advances in microfabrication technology facilitate artificial solid-state micro/nano-sized pores to be fabricated in an insulating membrane. By monitoring the images, ion currents, and force, as cells or molecules pass through a solid-state membrane sieve, it is possible to observe a wide range of phenomena involving genes, proteins, and cells [1], [4], [5]. The solid-state membrane sieve proves to be a very versatile tool for biophysics and biotechnology.

Among the solid-state membrane sieves, silicon-based microfabrication protocols for membrane structures with micro/nano-sized pores can give a well-defined pore geometry that can be defined as fine as the submicrometer level [4], [6]-[10]. Silicon-based membrane sieves, even though they are brittle materials, are not broken easily under typical hydrodynamic drive pressures, when designed properly. A highly tight and precise control of the size distribution of pores can be simply and precisely obtained using photolithography-based planar fabrication techniques. The pore geometry in planar microfabrication protocols can be easily designed in any arbitrary shape.

Si-rich Si_3N_4 is a typical Si-compound-based membrane material [4], [6]-[11]. It shows a level of stress relaxation from that of fully stoichiometric Si_3N_4. This is because the compositionally induced stress relaxation in Si-rich Si_3N_4 thin films gives strain relief at the molecular level due to tetrahedral

distortion, which is found in the substitution of Si for N in a tetrahedral unit [12], [13]. Due to this substitution, quite a large nonuniformity in the deposited film thickness occurs. This means that in case of an integration of a specific device on a membrane, like a resonator sensor, an unacceptable nonuniformity in the sensor sensitivity will take place. Moreover, the fabrication of membranes requires long periods of exposure of the Si_3N_4 films to such materials as aqueous KOH solutions; while the etch rate of the films in the solutions is quite low, the rate depends on the ratio of Si and N in the film [13], [14]. Furthermore, due to the nonuniformity of the thickness as well as the composition of the film, we also expect nonuniformity in the residual stress across the wafer surface, which may lead to mechanical structures with unequal properties [15], [16]. Thus, despite being complicated and difficult, optimization of the films for this membrane is a prerequisite.

A stoichiometric Si_3N_4 film with SiO_2 films of a stress compensator as a low-stressed insulator can be a good candidate for a sieve membrane with amenable properties [17]-[19]. This is because it has advantages of compatibility with standard complementary metal-oxide semiconductor (CMOS) processes, uniformity in thickness, and reliable integration ability with microsensors on the same membrane. Membrane sieves using a SiN/SiO_2 bilayer film have been reported [20]. A stoichiometric multilayer using the combination of both a stoichiometric Si_3N_4 layer and a SiO_2 layer may be preferable since it can provide residual stress reduction and electrical and chemical stability.

In this paper, we describe the design, fabrication, and characterization of stoichiometric, low-stressed, and standard IC-process-compatible membrane sieves or filters using stress-reduced $Si_3N_4/SiO_2/Si_3N_4$ triple-layer films. They have been applied to the separation of plasma and blood cells (for example, erythrocytes and leukocytes) from human whole blood. By employing an additional agarose gel matrix as a visualization matrix at the sieve plate, the absorption ability was greatly enhanced. Using the fabrication methods of the membrane sieves, the plasma from the human whole blood could be separated simply and rapidly.

II. Experiments

1. $Si_3N_4/SiO_2/Si_3N_4$ Membrane Design

The silicon-based microfilter membranes were prepared by combining depositions of the stress-reduced $Si_3N_4/SiO_2/Si_3N_4$ triple-layer films. The $Si_3N_4/SiO_2/Si_3N_4$-based micro membrane includes holes with diameters of 0.5 μm to 2 μm and a membrane with a thickness of 0.4 μm. Detailed

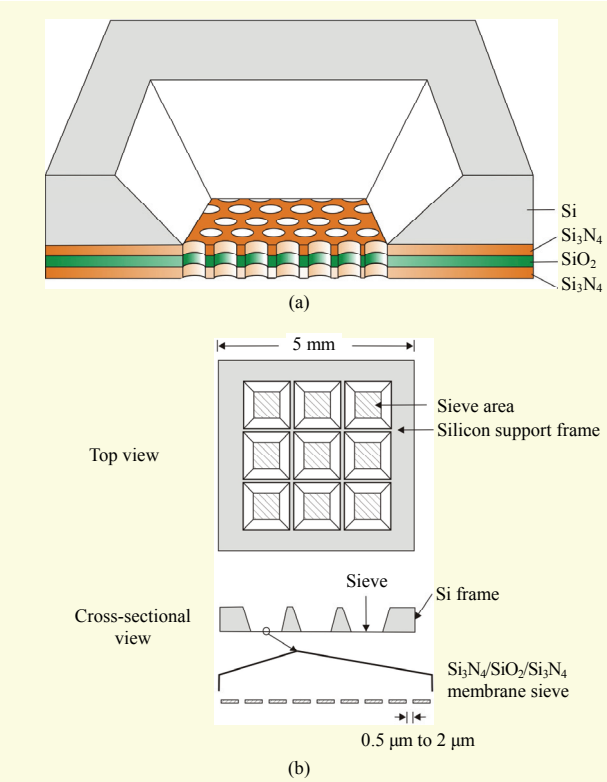

Fig. 1. Schematic diagram showing working principles of (a) $Si_3N_4/SiO_2/Si_3N_4$ membrane filter and (b) its structures.

schematic diagrams of the $Si_3N_4/SiO_2/Si_3N_4$ membrane sieves and its structures are shown in Figs. 1(a) and 1(b). For collecting the plasma from the membrane filter efficiently and rapidly, an agarose gel has been attached to holes on the membrane sieves. When using dielectric layers as membrane layers, the intrinsic stress must also be considered because intrinsic stress can occur in single layer or multilayer compositions and lead to membrane deformation or breakage [21]. Since residual stresses are generally much larger than other stresses like thermal stress, controlling the residual stresses in single layer and multilayer systems is crucial for membrane stability [21], [22]. Herein, we first compared the nonuniformity between the Si-rich and N-rich Si_3N_4 films by measuring the thickness values of the films. Then, we utilized the stress-reduced $Si_3N_4/SiO_2/Si_3N_4$ thin films, obtaining nearly zero stress films using the low-pressure chemical vapor deposition (LPCVD) to acquire compatibility with the following CMOS IC process. The results are summarized in Table 1. The thicknesses of the thin films deposited on a 6" Si wafer are measured at five points: top, bottom, right, left, and center sites using an ellipsometry.

Si_3N_4 thin films are deposited by LPCVD at 800ºC, in a mixture of $SiCl_2H_2$ and NH_3. At a pressure of 250 mTorr, the total gas flow is held constant at about 180 sccm. Films of

Table 1. Physical properties of designed stacked dielectric membranes when thickness of thin films is normalized to 1,000 Å.

Dielectric film	Standard dev. in thickness (Å)	Maximum deviation (Å)	Gas flow ratio at 800°C and 250 mTorr
Low-stressed Si_3N_4	39.62	113.76	150 : 30 sccm (SiH_2Cl_2 : NH_3) Dep. rate: 28 Å/min
Stoichiometric Si_3N_4	5.12	8.53	25 : 150 sccm (SiH_2Cl_2 : NH_3) Dep. rate: 20 Å/min
LPCVD SiO_2	24.22	62.11	300 sccm $Si(OC_2H_5)_4$ Dep. rate: 40 Å/min

varying compositions are produced by controlling the ratio of the $SiCl_2H_2$ flow to the total flow in the reactor from 0.14 to 0.83. The LPCVD furnace used in this study is a vertical thermal reactor with a wafer spacing of 10 mm. The wafers used are 150-mm diameter n-type Si (100), with a resistivity of 10 Ω cm. The thickness of the films used is in the range of 25 nm to 1,000 nm. The thickness of the thin films is fitted to 100 nm.

For a multilayer system, a combination of Si_3N_4 and SiO_2 was employed. The intrinsic stress measurement for the dielectric layers was performed by measuring the deformation of a 6" Si wafer after the deposition of a thin film. The results summarized in Table 2 show that the SiO_2 is compressive, whereas the Si_3N_4 is tensile. As such, the right combination of Si_3N_4 and SiO_2 can lead to acceptable resultant residual stress and good passivation for harsh chemical etchants. Therefore, stress-reduced stacked dielectric layers comprised of LPCVD Si_3N_4 (0.05 μm), LPCVD SiO_2 (0.3 μm), and LPCVD Si_3N_4 (0.05 μm) films were used, as shown in Table 2, based on the equations in the following paragraphs.

The resultant residual stress σ_r of a stacked membrane can be approximated by [23]

$$\sigma_r = \frac{\sigma_{Si3N4} d_{Si3N4} + \sigma_{SiO2} d_{SiO2} + \sigma_{Si3N4} d_{Si3N4}}{d_{Si3N4} + d_{SiO2} + d_{Si3N4}}, \quad (1)$$

$$\sigma_{Si3N4} = 1.2 + (E_{Si3N4} \times \alpha_{Si3N4} \Delta T) - (E_{Si3N4} / \nu \times \alpha_{Si3N4} \Delta T),$$
$$\sigma_{SiO2} = -0.27 + (E_{SiO2} \times \alpha_{SiO2} \Delta T) - (E_{SiO2} / \nu \times \alpha_{SiO2} \Delta T), \quad (2)$$

where d and σ are the thickness and intrinsic stress, respectively, of the different membrane layers. Rossi and others suggested an acceptable range for the resultant residual stresses as $-0.1\ \text{GPa} < \sigma_r < 0.1\ \text{GPa}$ [19].

Based on (1), the film parameters for the three layers were selected as shown in Table 2, and the resultant stress was calculated to be $-0.1\ \text{GPa} < \sigma_r < 0.1\ \text{GPa}$. The LPCVD Si_3N_4 layers had the highest intrinsic stress values (1.2 GPa tensile), while the oxide layer played a role in reducing the overall stress of the membrane. According to (1) and (2), the σ range facilitates a wide range of Si_3N_4 and SiO_2 thicknesses at a room temperature of 27ºC, as shown in Fig. 2(a). The acceptable stress region is shaded. Thus, the thickness of the stacked membranes is designed to have an acceptable resultant residual stress, which is marked with the filled circle in Fig. 2(a).

Table 2. Composition and their physical properties of multilayered dielectric membranes.

	Intrinsic stress (GPa)	Young' modulus, E (GPa)	Thermal expansion coefficient, α (10^{-6}/K)	Poisson ratio, ν
Si		160	2.6	0.22
SiO_2	–0.27	73	0.55	0.17
Stoichiometric Si_3N_4	1.2	323	2.8	0.25
Low-stressed Si_3N_4	< | 0.4 |			

2. Microfabrication of $Si_3N_4/SiO_2/Si_3N_4$ Membrane Sieves

The fabrication process was designed to be simple and suitable for mass production protocols. The fabrication process for the membrane sieve structures involves creating a Si device, as shown in Fig. 2(b). A double-sided polished Si (100) wafer with a six-inch diameter and about 630 μm in thickness was used as the substrate using the clean room facilities of the CMOS fabrication facilities at ETRI. After standard initial cleaning, Si_3N_4 (0.050 μm), SiO_2 (0.30 μm), and Si_3N_4 (0.10 μm), deposited using a LPCVD system (Centrotherm, Germany), were used to create a stress-reduced diaphragm and etch masking layer on both sides of the wafer. The thickness of the films is determined to be thin considering the reduced stresses after measuring their residual stresses, as previously reported [23], [24]. The insulating layers on the bottom of the Si wafers were patterned using a typical photolithographic system of an i-line stepper (Nikon NSR2205, Japan) and etched down to the silicon using the RIE system. The upper $Si_3N_4/SiO_2/Si_3N_4$ membrane layer (0.4 μm) was patterned by photolithography and dry-etched using the RIE system onto the Si substrate. The alignment of the patterns of the membrane holes on the top of the wafer with that of the membrane was accomplished by a bottom side alignment using a mask aligner (MA6/BA6, SussMicroTec Co.). To form the 0.4-μm-thick stress-reduced $Si_3N_4/SiO_2/Si_3N_4$ diaphragm, the bottom of the Si wafer was wet-etched in a KOH solution (26% weight, 85ºC) for about ten hours through the entire wafer level using a

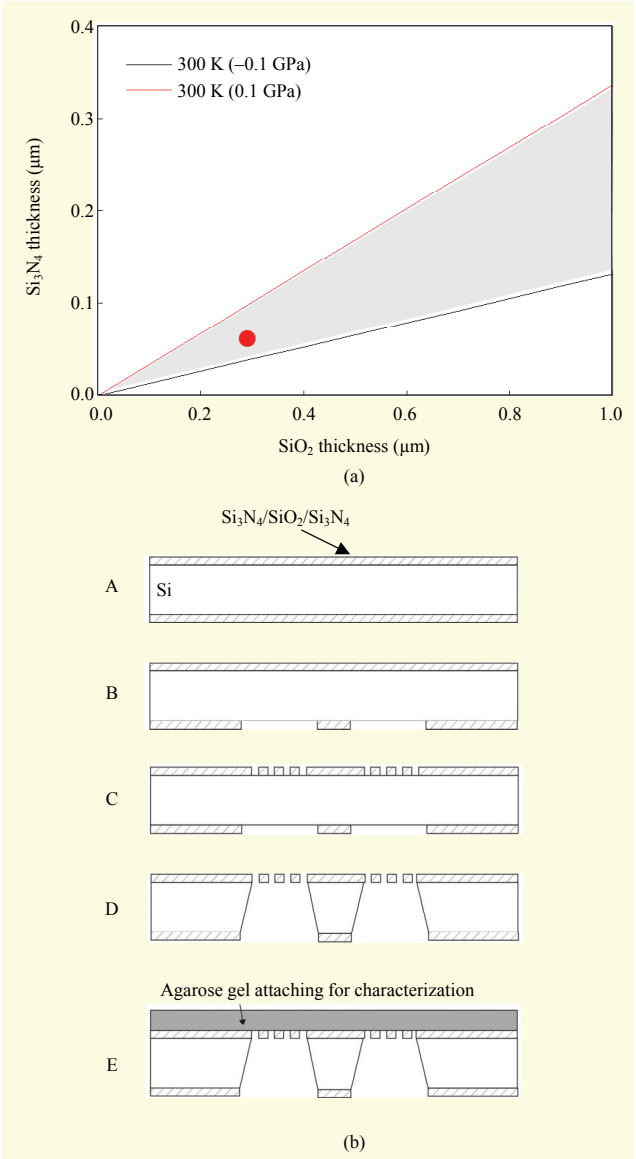

Fig. 2. (a) Calculation of Si_3N_4 thickness (top plus bottom layers) vs. SiO_2 thickness to achieve $|\sigma|<0.1$ GPa and (b) sequential procedures for fabrication of $Si_3N_4/SiO_2/Si_3N_4$ membrane sieves.

custom-made etching manifold that completely sealed the top part and allowed only the bottom part of the Si to be etched. The wafer was then diced into discrete chips. Photographs of the process results are shown in Fig. 3. Figures 3(a), 3(b), and 3(c) show the top view of the membrane sieves, the bottom view of the membrane sieves, and the top view of the sieves attached to the agarose gel matrix in a 3×3 array, respectively. Figure 3(d) shows an SEM photograph of the holes formed periodically on the $Si_3N_4/SiO_2/Si_3N_4$ membrane with about a 2-μm diameter.

In these membrane sieves, the fill factor, which means the area ratio of pores to membrane, was 18%. However, the fill

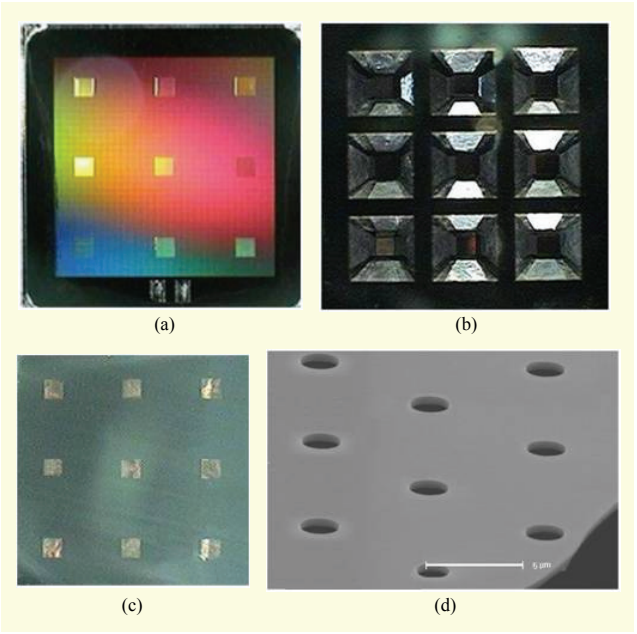

Fig. 3. Photographs of $Si_3N_4/SiO_2/Si_3N_4$ membrane filter (5 mm× 5 mm): (a) top membrane part, (b) bottom well part, (c) top membrane attached with agarose gel, and (d) magnified views on membrane sieves with 2-μm diameter.

factor can be easily and simply expandable by changing the number and size of the pores at the photomasks.

3. Characterization of Plasma Penetration Using Membrane Sieves

Agarose, a polysaccharide derived from red seaweed, is a typical material used in chromatography and electrophoresis. It is a kind of porous nano-sized sieve having strong capillary hydraulic permeability like a diaper [25]. Because only a little amount of plasma can be obtained through filtration, it is difficult to obtain with a conventional pipette. We attached small gel blocks on the backside of the microfabricated membrane holes, inducing a rapid absorption of plasma into the gel block. The use of hydrogel can contribute to an increase in the extraction speed of the plasma. It can be a solution for reducing the clogging effects in the flow since it takes about 30 min to saturate the filter due to clogging [26].

One percent (w/v) agarose gel (Gibco BRL) was prepared by boiling the agarose powder with deionized water. The melted agarose was poured into a dish making a 1-mm-thick layer and was then allowed to be solidified at room temperature. Gel blocks were obtained by cutting the layer into small 5-mm× 5-mm×1-mm blocks.

Above all, by penetrating the membrane with red dye in deionized water, we observed the functioning of the sieve and the resulting color changes on the agarose gel. To monitor the

plasma passage by observing fluorescence images, we prepared a blood plasma sample, which was collected through the centrifugal separation of human capillary blood and twice-diluted with a phosphate buffered saline solution (0.1 M PBST, pH 7.4, Tween 0.1%, 1 mM EDTA). Fluorophore Alexa TM 488-labeled hemoglobin (100 μg/mL) was added to the prepared blood plasma and tested. The sieving products were observed immediately after 10 min with a sample loading under a fluorescence microscope with an exposure of 5.9 s. Finally, a gel block was attached to the backside of the filter membrane, and 5 μL of whole capillary human blood, which had been collected from a normal man's finger and treated with an anti-coagulant of ethylenediaminetetraacetic acid (EDTA), was applied to the filter. The hematocrit of the whole blood was around 45%. The gel block was removed out of the sieve membrane after several minutes. Gel blocks were melted down by boiling with a sodium dodecyl sulfate-polyacrylamide gel electrophoresis (SDS-PAGE) loading buffer, and the existence of proteins was analyzed through SDS-PAGE, followed with staining using Coomasssie Brilliant Blue R-20 (Sigma, Co.), as previously described [27].

III. Results and Discussion

1. Properties of $Si_3N_4/SiO_2/Si_3N_4$ Multilayer Membrane Sieves

The mechanical, electrical, and chemical stability of the membrane is basically caused by the material and preparation processes. We first measured the nonuniformity of the thickness of the Si_3N_4 thin film as a function of the $SiCl_2H_2/NH_3$ gas ratio in the total flow (~180 sccm) in the reactor from 0.14 to 0.83 at a temperature of 800ºC and a pressure of 250 mTorr using LPCVD. The results are summarized in Table 1, which show that the residual stress of nonstoichiometric Si_3N_4 films can be controlled; however, the nonuniformity of the films is quite large. Lau and others have reported that for Si-rich SiN film deposition on a five-inch silicon wafer, nonuniformity of the deposition rate and a refractive index of around ± 10% are obtained while the film residual stress remains low (< 50 MPa) [16]. The results of our experiment are well in accord with earlier results. This is because the compositionally-induced stress relaxation in Si-rich Si_3N_4 thin films provides strain relief at the molecular level due to tetrahedral distortion, which is caused by the substitution of Si for N in the tetrahedral unit [12], [14]. Due to this substitution, quite a large nonuniformity in the deposited film thickness occurs. This seems to indicate that in the specific device integration on a membrane, such as a resonator sensor, some degradation in sensor sensitivity will take place. Because of the nonuniformity in the thickness, as well as in the composition of the film, we also see the nonuniformity in the residual stress across the wafer surface, which will lead to mechanical structures with unequal properties. Lau and others have also reported that at a high temperature (≥750ºC), for Si-rich film deposition, the consumption effect leads to thickness nonuniformity of around ±30% along the load [16], whereas the stoichiometric Si_3N_4 films show a high tensile residual stress; however, the nonuniformity is very low. As for stoichiometric SiO_2, the residual stress and nonuniformity of the films seems to be acceptable.

Si-rich Si_3N_4 films are known to display a large hysteresis loop in the capacitance-voltage curve and a large flat-band shift with respect to the polarity of the bias voltage. This is because Si dangling bonds, which can trap either electrons or holes in Si-rich Si_3N_4 films, are dominant defects. However, the Si dangling bonds are greatly reduced in N-rich films, that is, stoichiometric Si_3N_4, and the dominant residual traps are only hole traps [16], [17]. Thus, the electrical properties of the stoichiometric Si_3N_4 film will be enhanced and preferable.

Through the fabrication processes, the stoichiometric Si_3N_4 film shows excellent chemical endurance to harsh chemicals such as KOH, TMAH, HF, solvents, HNO_3, HCl, and H_2SO_4. As for KOH solution as a Si etchant, the 100-nm-thick stoichiometric Si_3N_4 membrane could endure the solution for ten hours at 85ºC. However, the Si-rich Si_3N_4 membrane could not endure and showed some nonuniformity in the etch rates.

Thus, combining the advantages of stoichiometric Si_3N_4 and SiO_2 films, a stoichiometric $Si_3N_4/SiO_2/Si_3N_4$ multilayer membrane that is very flat mechanically stress-reduced and possesses electrically- and chemically-stable properties would be a good solution for a stable micro/nano sieve membrane.

2. Application of Multilayer Membrane Sieve in Blood Plasma Separation

Using the $Si_3N_4/SiO_2/Si_3N_4$ membrane sieves as shown, we investigated the sieving performances of the chip for red dye solutions and whole human blood. The testing results were scrutinized using the optical or fluorescence images. The agarose gel was utilized for efficient collection and visualization of the plasma from the whole human blood. In addition, components of the absorbed plasma through the agarose gel were analyzed in terms of their molecular sizes using gel electrophoresis.

The separation speed was improved by combining agraose gel having strong capillary hydraulic permeability with the membrane sieves [25], [28]. Otherwise, the flow would be delayed by the clogging of accumulated cells. First, we confirmed the penetration of liquid through the filter

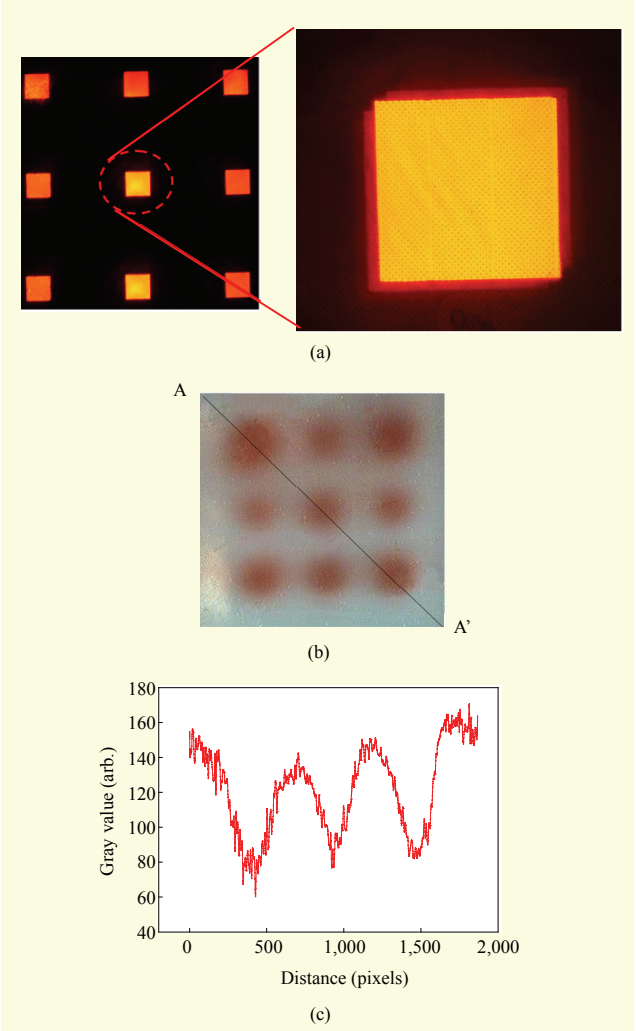

Fig. 4. $Si_3N_4/SiO_2/Si_3N_4$ membrane sieves containing red dye solutions: (a) magnified version, (b) absorption patterns on agarose gel attached to silicon membrane filter for a plasma sieving after 2 min, and (c) a gray value plot profile along with diagonal line (AA') for image in (b).

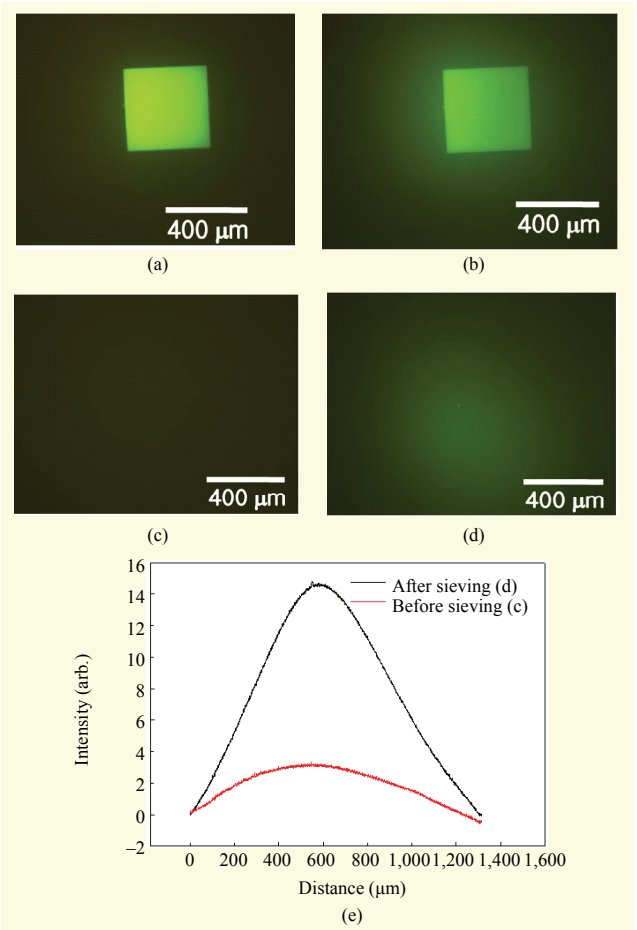

Fig. 5. Fluorescence photographs showing blood plasma penetration through a triple-layer membrane sieve: (a) from the start, (b) after 10 min, (c) agarose gel top surface at removing sieves after 10 min and showing penetration of blood plasma, (d) agarose gel top surface before contact, and (e) gray value plot comparison between (c) and (d).

membrane by observing the passing of red dye. After loading the red dye solution into the membrane sieves in a 3×3 array attached with agrarose gel, as shown in Fig. 4(a), we checked the color changes caused by the red dye solution that was absorbed into the agarose gel block. We can see the pores on the membrane very clearly in Fig. 4(a), which means good contact between the membrane sieves and agarose gel. After only two minutes, the red dye permeated into the agarose gel in large amounts, as shown in Fig. 4(b). There was no detectable damage or breakage in the filter membrane after the experiments. For more visualization, a gray value plot profile along with a diagonal line (A-A') on the image in Fig. 4(b) is drawn in Fig. 4(c). Therefore, it was evident that the membrane sieves could let the liquid sample flow through itself.

Second, we observed the blood plasma penetration performance of the membrane sieves. Fluorescence photographs showing whether the twice-diluted human blood plasma with PBST solution containing hemoglobin labeled with fluorophore Alexa TM 488 beads passed through the membrane sieves are shown in Fig. 5. In the initial loading of the human blood plasma, the edge of the micro well was clear and no exudation is found. However, the fluorescence photograph taken after ten minutes shows that there was some blurring of the edge line and gradients of fluorescent color appeared. The gradients of an optical signal are increased as a function of time. After ten minutes, we detached the membrane sieves from the agarose gel, took fluorescence photographs of the agarose gel surface, and then compared them with the surface before loading, as shown in Figs. 5(c), 5(d), and 5(e). Even though there is a background signal caused by the self fluorescence of the gel, the steep intensity increase of the

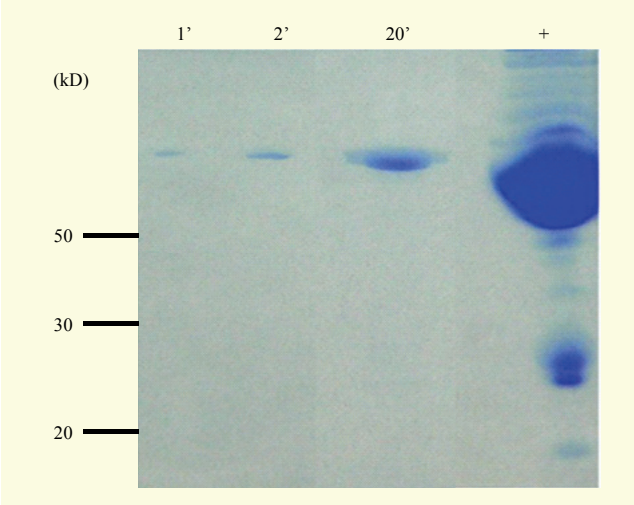

Fig. 6. SDS-PAGE analysis of proteins absorbed into gel blocks in plasma exuded through membrane sieve. The gel blocks were taken after different sieving times (1 min, 2 min, 20 min). The gel was mixed with equal volume of loading buffer, boiled for melting, and loaded along with the size standards and 1 μL of human plasma (lane +).

fluorescence signal means that the exudation of the blood plasma in the membrane sieves is working well.

Next, we applied the membrane sieves for the extraction of plasma out of whole human blood, shown in Fig. 6. For this, we measured the whole blood sample volume using a micropippet to be 5 μL and put it in the well. After separation of the plasma, we tried to collect the plasma using a micropippet again. It is difficult to measure the plasma volumes precisely because collected plasma volumes are very small, there is wetting on the chip surface, and some plasma is absorbed into the gel. Thus, we measured again the whole plasma remaining in the well, and it was about 4 μL. We thought the collected plasma from the whole blood would be about 1 μL. The passing of plasma through the membrane sieve was revealed through the detection of plasma protein in the gel block. Figure 6 shows the SDS-PAGE analysis of the proteins absorbed in the gel block. We could detect serum albumin protein (~65 kD), the most abundant among the plasma proteins, after one minute of filtration. The filtration of whole human blood increased as a function of working time and saturated at about five minutes (data not shown). There was no detectable loss of integrity of the membrane sieves after several usages, and we could not find any blood cells on the agarose gel block through a light microscope after filtration, which means that only the plasma passed through the membrane sieves. As for the hemolysis, because hemoglobin is the major protein of RBC (> 90% of dry weight), any tiny amount of hemolysis makes the plasma (or serum) reddish. According to the figure of filtrate on the agarose gel, we could see that detectable amount of hemolysis did happen during the filtration. However, there was little amount of hemoglobin when the filtrate was analyzed by SDS-PAGE. Two types of hemoglobin monomers range around 15 kD. Therefore, we can conclude that hemolysis happens at a negligible level.

Although we could apparently observe the transferring of the plasma without attaching agarose gels, the amount of obtained plasma was too little to harvest for further analyses because of substantial accumulation of blood cells in the capillary force-driven microfluidic blood flow. The separation speeds seemed to be enhanced through the capillary sieving effect due to the porosity of hygroscopic agarose gel. In such a measurement system, it is important to keep close and tight contact between the membrane sieves and agarose gel matrix, for reliable separation speeds and good separation efficiency. Currently, the volume of plasma that can be harvested by our membrane filter is several hundreds of nanoliters. In future work, our research will focus on increasing the separation efficiency by increasing the fill factor, finding multistacking membrane structures to reduce clogging, and designing structure modifications physically and chemically to facilitate the flow rate. We speculate that the results could be applied to several nanofabricated biosensors, considering that most of the current biosensors are aimed at consuming tiny amounts of samples [29]-[32]. Furthermore, the fabricated microstructures could also be applicable to cell cytotoxicity analysis systems or cell-based biosensor systems [33]-[35].

IV. Conclusion

We have designed and fabricated a novel stoichiometric $Si_3N_4/SiO_2/Si_3N_4$ triple-layer membrane sieve device. The $Si_3N_4/SiO_2/Si_3N_4$ micro/nano-sized membrane sieves are designed to be very flat, very thin, mechanically stress-reduced, and stable in their electrical and chemical properties. All insulating materials are deposited stoichiometrically using an LPCVD system. The $Si_3N_4/SiO_2/Si_3N_4$ membranes with a thickness of 0.4 μm have pores with diameters of 0.5 μm to 2 μm. The stoichiometric $Si_3N_4/SiO_2/Si_3N_4$ multilayer membrane can be a good alternative for Si-rich low-stressed Si_3N_4 membranes in terms of electrical and chemical stability and compatibility with the following processes for the integration of microdevices. To create pores in the membrane, we utilized typical semiconductor process protocols of i-line steppers and dry/wet-etching protocols for mass production and precise control in terms of the size, shape, and fill factor of the pores. This microfabrication protocol for a membrane filter is compatible to the CMOS IC fabrication protocols and feasible for integrating with microsensors.

The membrane sieves were applied to the plasma penetration

in whole human blood by simply attaching an agarose gel matrix, which can provide a capillary sieving effect due to the nano-sized porosity. In addition, the separation performances are experimentally demonstrated using a liquid dye solution, twice-diluted plasma with PBST solutions, and real whole human blood. The membrane sieves penetrated the red dye solutions and twice-diluted plasma. The sieves can selectively extract plasma from whole human blood at an apparently detectable level. The membrane sieves are useful in cell separation and analysis system or cell-based biosensor applications in analytical chemistry and the field of separation science.

References

[1] C. Dekker, "Solid-State Nanopores," *Naute Nanotechnol.*, vol. 2, Apr. 2007, pp. 209-215.

[2] J. Fu, P. Mao, and J. Han, "Artificial Molecular Sieves and Filters: A New Paradigm for Biomolecule Separation," *Trend in Biotechnology*, vol. 26, no. 6, Apr. 2008, pp. 311-320.

[3] R. Reis and A. Zydney, "Membrane Separations in Biotechnology," *Current Opinion Biotechnol.*, vol. 12, 2001, pp. 208-211.

[4] J. Li et al., "Nanoscale Ion Beam Sculpting," *Nature*, vol. 412, no. 166, July 2001, pp. 166-169.

[5] T. Xu et al., "A Cancer Detection Platform Which Measures Telemerase Activity from Live Circulating Tumor Cells Captures on a Microfilter," *Cancer Research*, vol. 70, no. 16, Aug. 2010, pp. 6420-6426.

[6] C.J.M. Rijn, G.J. Veldhuis, and S. Kuiper, "Nanosieve with Microsystem Technology for Microfilteration Applications," *Nanotechnol.*, vol. 9, Feb. 1998, pp. 343-345.

[7] X. Yang et al., "Micromachined Membrane Particle Filters," *Sensors and Actuators*, vol. 73, Jan. 1999, pp. 184-191.

[8] H.D. Tong et al., "Silicon Nitride Nanosieve Membrane," *Nano Lett.*, vol. 4, no. 2, Feb. 2004, pp. 283-287.

[9] S.H. Ma et al., "An Endothelial and Astrocyte Co-culture Model of the Blood-Brain Barrier Utilizing an Ultra-thin, Nanofabricated Silicon Nitride Membrane," *Lab on a Chip*, vol. 5, Jan. 2005, pp. 74-85.

[10] M.J.K. Klein et al., "SiN Membranes with Submicrometer Hole Arrays Patterned by Wafer-Scale Nanosphere Lithography," *J. Vacuum Sci. Technol. B:Microelectron. Nanometer Structures*, vol. 29, no. 2, Feb. 2011, pp. 021012-1-5.

[11] A.A. Patel and H.I. Smith,"Membrane Stacking: A New Approach for Three-Dimensional Nanostructure Fabrication," *J. Vacuum Sci. Technol. B:Microelectron. Nanometer Structures*, vol. 25, no. 6, June 2005, pp. 2662-2664.

[12] S. Habermehl, "Stress Relaxation in Si-Rich Silicon Nitride Thin Films," *J. Appl. Physics*, vol. 83, no. 9, May 1998, pp. 4672-4677.

[13] J.G.E. Gardeniers and H.A.C. Tilmans, "LPCVD Silicon-Rich Silicon Nitride Films for Applications in Micromechanics," *J. Vacuum Sci. Technol. A*, vol. 14, no. 5, Sept. 1996, pp. 2879-2892.

[14] P.T.Boyer, L.Jalabert, and L.Masarotto, "Properties of Nitrogen Doped Silicon Films Deposited by Low-Pressure Chemical Vapor Deposition from Silane and Ammonia," *J. Vacuum Sci. Technol. A*, vol. 18, no. 5, Sept. 2000, pp. 2389-2393.

[15] G.T.A. Kovacs, *Micromachined Transducers Sourcebook*, NY, US:WCB/McGraw-Hill, 1998.

[16] W.S. Lau, S.J. Fonash, and J. Kanicki, "Stability of Electrical Properties of Nitrogen-Rich, Silicon-Rich, Stoichiometric Silicon Nitride Films," *J. Appl. Physics*, vol. 66, no. 6, Sept. 1989, pp. 2765-2767.

[17] S.H. Hong et al., "Improvement of the Current-Voltage Characteristics of a Tunneling Dielectric by Adopting a $Si_3N_4/SiO_2/Si_3N_4$ Multilayer for Flash Memory Application," *Appl. Physics Lett.*, vol. 87, no. 15, Oct. 2005, pp.152106-1-3.

[18] A.J. Storm et al., "Fabrication of Solid-State Nanopores with Single-Nanometre Precision," *Nature Materials*, vol. 2, Aug. 2003, pp. 537-540.

[19] C. Rossi, P.T. Boyer, and D. Esteve, "Realization and Performance of Thin SiO_2/SiNx Membrane for Microheater Applications," *Sensors and Actuators A*, vol. 64, no. 3, Jan. 1998, pp. 241-245.

[20] M.Y. Wu et al., "Formation of Nanopores in a SiN/SiO_2 Membrane with an Electron Beam," *Appl. Physics Lett.*, vol. 87, no. 11, Sept. 2005, pp.113106-1-3.

[21] C. Mastrangelo, and W. Tang, "Semiconductor Sensor Technologies," *Semiconductor Sensors*, S. Sze (Ed.), Wiley, 1994, pp. 17-95.

[22] H. Low, M. Tse, and M. Chiu, "Thermal Induced Stress on the Membrane in Integrated Gas Sensor with Micro-heater," *Proc. IEEE Hong Kong Electron Devices Meeting*, 1998, pp.140-143.

[23] D.S. Lee et al., "Bulk-Micromachined Submicroliter-Volume PCR Chip with Very Rapid Thermal Response and Low Power Consumption," *Lab on a Chip*, Mar. 2004, pp. 401-407.

[24] D.S. Lee et al., "A Temperature-Controllable Microelectrode and Its Application to Protein Immobilization," *ETRI J.*, vol. 29, no. 5, Oct. 2007, pp. 667-669.

[25] S. Hattori et al., "Structure and Mechanism of Two Types of Micro-pump Using Polymer Gel," *Proc. MEMS*, 1992, pp. 110-115.

[26] V. VanDelinder and A. Groisman, "Separation of Plasma from Whole Human Blood in a Continuous Cross-Flow in a Molded Microfluidic Device," *Analytic Chemistry*, vol. 78, June 2006, pp. 3765-3771.

[27] J. Sambrook and D.W. Russell, *Molecular Cloning: A Laboratory Manual*, 3rd ed., Cold Spring Harbor, NY: Cold Spring Harbor Laboratory Press, 2001.

[28] Y.H. Choi, S.S. Lee, and K.W. Chung, "Microfluidic Actuation and Sampling by Dehydration of Hydrogel," *Biochip J.*, vol. 4, no. 1, Apr. 2010, pp. 63-69.
[29] D. Erickson et al., "Nanobiosensors: Optofluidic, Electrical and Mechanical Approaches to Biomolecular Detecton at the Nanoscale," *Microfluid Nanofluidics*, vol. 4, no. 1, Sept. 2008, pp. 33-52.
[30] G.A.Urban and T.Weiss, "Hydrogel for Biosensors," *Hydrogel Sensors and Actuators, Springer Series on Chemical Sensors and Biosensors 6*, S. Gerlach and K.-F. Arndt (Eds.), Springer-Verlag, Berlin, 2009.
[31] N. Massad-Ivanir et al., "Construction and Characterization of Porous SiO_2/Hydrogel Hybrids as Optical Biosensors for Rapid Detection of Bacteria," *Adv. Functional Materials*, vol. 20, June 2010, pp. 2269-2277.
[32] H. Uehara et al., "Size-Selective Diffusion in Nanoporous but Flexible Membrane for Glucose Sensors," *ACS Nano*, vol. 3, no. 4, Mar. 2009, pp. 924-932.
[33] S. Howorka and Z. Siwy, "Nanopore Analytics: Sensing of Single Molecules," *Chem Soc Rev*, vol. 38, June 2009, pp. 2360-2384.
[34] P. Wang et al., "Cell-Based Biosensors and Its Applications in Biomedicine," *Sens Actuators B:Chem*, vol. 108, July 2005, pp. 576-584.
[35] Z. Wang et al., "High-Density Microfluidic Arrays for Cell Cytotoxicity Analysis,"*Lab Chip*, vol. 7, Apr. 2007, pp. 740-745.

Dae-Sik Lee is a principal researcher in the BioMED Team at ETRI, Daejeon, Rep. of Korea. He received his BS, MS, and PhD in electronic engineering from Kyungpook National University in 1995, 1997, and 2000, respectively. He also obtained his PhD in nano-science and nano-engineering in the Department of Electronic and Photonic System, Waseda University, 2009. His research interests include the design, simulation, fabrication, and characterization of BioMEMS devices and systems, microfluidic devices and systems, actuators and biochips, lab-on-a-chip, optics, and nano-engineering for biosensors.

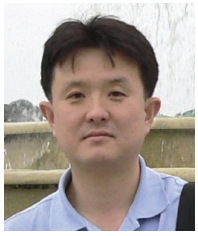

Yo Han Choi received his PhD from the Department of Life Science in Pohang University of Science and Technology (POSTECH), Rep. of Korea, in 2001. He has researched the development of anti-HIV drugs, cell biology, and protein chemistry using biochemical and molecular biological methods. After several years of research as a post-doctoral research fellow in the Department of Mechanical Engineering in POSTECH and the University of Alberta, Canada, and as a research professor in the Department of Mechanical Engineering at Korea Advanced Institute of Science and Technology (KAIST), he is currently working as a senior researcher in ETRI. His research interests are actuation systems, biochips including protein chips and cell chips, and manipulation of biomolecules using MEMS technology.

Yong Duk Han studied biochemical engineering and bionanotechnology and received his BS and MS in 2008 and 2010, respectively, at Ajou University, Rep. of Korea. He is currently studying for his PhD at Ajou University. His research interests reside in the biosensors, lab chips, and the fabrication of bioinspired nanoscale interfaces and nano-biotechnological applications.

Hyun C. Yoon received his BS in biotechnology from Korea Advanced Institute of Science & Technology (KAIST), and his MS and PhD in biological sciences from KAIST. His research involved electrochemical biosensor development. From 2001 to 2003, Dr. Yoon was a senior researcher at ETRI, Rep. of Korea. His research focused on biomicropatterning and bioanalytical lab-on-a-chip development. Dr. Yoon is presently an associate professor of molecular science and technology at Ajou University, Rep. of Korea, and is working on nano-biotechnology and biosensor development.

Shuichi Shoji received his BS, MS, and PhD in electronic engineering from Tohoku University in 1979, 1981, and 1984, respectively. He had been with Tohoku University as a research associate and associate professor from 1984 to 1992. In 1994, he moved to Waseda University as an associate professor. He is currently a professor in the Department of Electronic and Photonic Systems, specializing in nano-science and nano-engineering, Waseda University. His current interests are micro/nano devices and systems for chemical/bio applications.

Mun Youn Jung is currently the director of the BioMED team at ETRI, Daejeon, Rep. of Korea.